Desalination and Water Treatment
www.deswater.com

doi: 10.1080/19443994.2013.848668

52 (2014) 5061–5067
July

Taylor & Francis
Taylor & Francis Group

Understanding PVDF ultrafiltration membrane fouling behaviour through model solutions and secondary wastewater effluent

Rui Miao, Lei Wang*, Ling Feng, Zi-Wen Liu, Yong-Tao Lv

School of Environmental and Municipal Engineering, Xi'an University of Architecture and Technology, Yan Ta Road, No. 13, Xi'an 710055, China
Tel./Fax: +86 029 8220 2729; email: wl0178@126.com

Received 7 May 2013; Accepted 11 September 2013

ABSTRACT

In this work, we investigated the fouling behaviour of polyvinylidene fluoride (PVDF) ultrafiltration (UF) membranes. PVDF UF membranes prepared by the phase separation method were used to filter four sample solutions, namely bovine serum albumin (BSA), sodium alginate (SA), humic acid (HA) and secondary wastewater effluent organic matter (EfOM). Fouling experiments were carried out in a dead-end filtration set-up. Besides, the removal rate of dissolved organic carbon, the distribution of molecular weight and the permeability of feed water were inspected through direct comparison of the surface morphology of an uncontaminated and a contaminated membrane. The different fouling behaviours of BSA, SA, HA and EfOM were noted. It was found that the flux of the BSA-fouled membrane declined sharply at the initial filtration stage, but a more significant flux decline occurred for the SA-fouled membrane at the later filtration stage. For the HA-fouled membrane, a gradual flux decline was observed throughout the whole filtration stage. In three samples, HA generated the smallest flux decline rate and BSA produced the largest rate. Moreover, the fact that it took a very short time to approach about 50% flux reduction indicated that membrane fouling mainly occurred in the initial filtration stage. It was also found that the gel-layer structure on the membrane surface was strongly associated with the fouling behaviour of the membrane.

Keywords: Polyvinylidene fluoride; Fouling behaviour; Foulant types

1. Introduction

With increasing water source pollution and water quality requirements [1–3], membrane technology is extensively used in particular in advanced wastewater reclamation and drinking water reuse. However, the main obstacle for efficient application of the membrane technique is membrane fouling, which can cause a decrease in membrane flux and performance, leading to reduced productivity, deterioration of permeate quality, increased energy consumption and treatment cost, as well as shorter membrane lifespan [4–6]. Therefore, it is essential to learn more about the reasons for membrane fouling.

*Corresponding author.

Presented at the Conference on Water Resources and Urbanization Development, 26–27 September 2012, Tianjin, China

A considerable number of studies on membrane fouling have focused on identifying advantage foulants that could cause membrane fouling [7–9]. In the early 1970s, Rebhun et al. reported that the mass percentages of carbohydrate, protein and humus substances in city sewage secondary effluent were 12, 22 and 40–50%, respectively [10]. Moreover, in wastewater treatment and advanced water reclamation, it has been confirmed that dissolved organic matters, such as polysaccharides, proteins and natural organic matter, were the major foulants for membrane fouling [4,11,12]. Consequently, to understand better the effects of foulant types on membrane fouling, many existing studies used bovine serum albumin (BSA), sodium alginate (SA) and humic acid (HA) as surrogates for protein, polysaccharides and humus substances to analyse the mechanisms of membrane fouling [13,14]. Of course, many studies also concentrated on the membrane fouling by actual wastewater [7,8,15]. However, there is no consensus on the effect of foulant type on membrane fouling behaviour. Kimura [16] reported that the hydrophilic fraction of the organic matter was responsible for the irreversible fouling regardless of the type of membrane or organic matter. This result was confirmed by Her et al., who regarded hydrophilicity and polysaccharide-like substances as possible foulants for membrane fouling [12,17]. In contrast, other researchers reported that membrane fouling was attributed to high hydrophobic fractions (humic substances) in wastewater [18–20]. Protein has also been regarded as one of the main foulants for membrane fouling [7]. Susanto [21] showed that the synergistic effect between polysaccharide and protein resulted in a stronger reduction in flux than individual solutes under the same conditions [21]. It was also reported that the synergy between hydrophobic and hydrophilic natural organic matter attributed membrane fouling [13]. However, no significant synergistic effect was observed in the experimental results with the HA/SA mixtures [8]. All of these inconsistent findings may have resulted from differences in membrane properties, raw water quality, experimental artefacts and extraction procedures. Consequently, it is important to investigate further the effects of foulant type on membrane fouling under specific conditions.

In this study, one of the most commonly used membranes, polyvinylidene fluoride (PVDF) ultrafiltration (UF) [22], was prepared by the phase separation method and membrane fouling experiments were carried out with BSA, SA, HA and secondary wastewater effluent (effluent organic matter (EfOM)). The surface morphology of clean and fouled membranes was investigated by atomic force microscope (AFM). The dissolved organic carbon (DOC) removal rate and molecular weight distribution of feed water and permeate were also used to reveal the fouling behaviour of the membrane. The aim was to provide a visual insight into the fouling behaviour of BSA, SA, HA and EfOM to provide a theoretical basis for the prevention and control of membrane fouling.

2. Materials and methods

2.1. Foulants

BSA ($M_w = 67$ kDa, Shanghai blue season biological Co. Ltd., Shanghai, China), SA (Shanghai Guangfu Reagent Co., Shanghai, China) and HA (Shanghai Guangfu Reagent Co., Shanghai, China) (all in powder form) were used to represent the protein, polysaccharide and humus substances in wastewater. The BSA and SA stock solutions (2 g/L) were prepared by dissolving the foulant in deionized (DI) water with no pH adjustment. The HA stock solution (2 g/L) was prepared by dissolving 2 g HA in 0.1 mol/L (100 ml) NaOH solution and metering the volume with DI water, which was carried out after vigorous agitation for 24 h. Next, the SA and HA solutions were filtered with a 0.45 μm microfiltration membrane to remove particles and insoluble matter. All the stock solutions were stored in sterilized glass bottles at 4˚C. Prior to a fouling test, the DOC concentration of each stock solution should be diluted to 6.4 mg/L, which is equal to the DOC concentration in EfOM.

The EfOM from the fourth sewage treatment plant in Xi'an (China) was used as the actual wastewater. It was filtered with a 0.45 μm microfiltration membrane and stored at 4˚C before use.

2.2. Preparation of PVDF UF membranes

The flat-sheet PVDF UF membranes used in this study were home-prepared by the phase separation method as described previously [23]. Briefly, the preparation process was as follows: PVDF (Solef 1015; Solvay Advanced Polymers Co., USA) and PVDF (Sichuan Jiafeng Chemical Reagent Co., China) (blend ratios 16/4 (wt/wt)) were dissolved in dimethylacetamide (80 wt%; Tianjin Fucheng Chemical Reagent Co., China) and mixed for 24 h at 60˚C under vigorous stirring. The polymer solution was allowed to stand for 1 day to allow air bubbles to escape. The resulting homogeneous polymer solution was uniformly spread onto a glass plate using a casting knife with a gap of 100 μm. Next, the glass plate with the cast solution was immersed immediately

into a DI water bath set at a temperature of 60˚C. The formed solid membranes were immersed in DI to remove residual solvent for 5–7 days. To minimize the presence of water in the polymer, PVDF and other additives were dried at the desired temperature in a vacuum oven.

2.3. Membrane filtration set-up and filtration experiments

A laboratory-scale dead-end membrane filtration set-up was used for the filtration experiments as described previously [24]. The filtration set-up is shown in Fig. 1. A membrane sample with an effective filtration area of 28 cm^2 was set up on the bottom of a stirred dead-end cell. The stirred cell was also used as a reservoir to hold the feed solution. A compressed N_2 cylinder was used to provide pressure for the membrane sample. The pressure was kept constant during the filtration time by a pressure gauge. An electronic balance was connected with the data register (computer) to continuously monitor the permeate flux online. The membrane water flux was calculated according to Eq. (1):

$$J = \frac{V}{A \cdot t} \quad (1)$$

where J is the membrane flux (in L/m^2 h), V is the permeate fluid volume (in L), A is the effective membrane area (in m^2) and t is filtration time (in h).

One clean membrane was used for each fouling filtration. The filtration protocol for BSA, SA, HA and EfOM was as follows. The membrane was first precompacted with DI water under 0.15 MPa until the membrane permeate flux reached a stable value. Then, the transmembrane pressure was reduced to 0.1 MPa and the membrane was stabilized with DI water for 30 min to reach a stable permeate flux, which was evaluated in terms of the pure water flux of membrane (J_0). The aim of these steps was to ensure that permeate flux changes during fouling filtrations were solely attributed to the foulants, not to any structural changes caused by membrane compaction and swelling [25]. Finally, the feed solution with desired DOC was filtered through the membrane under 0.1 MPa for 2 h. The changes in permeate flux were monitored continuously throughout all fouling experiments and the corresponding flux decline curves were used to assess the membrane fouling trend. All fouling experiments were conducted at 20˚C and at least four replicates of the fouling experiments were carried out for each type of foulant.

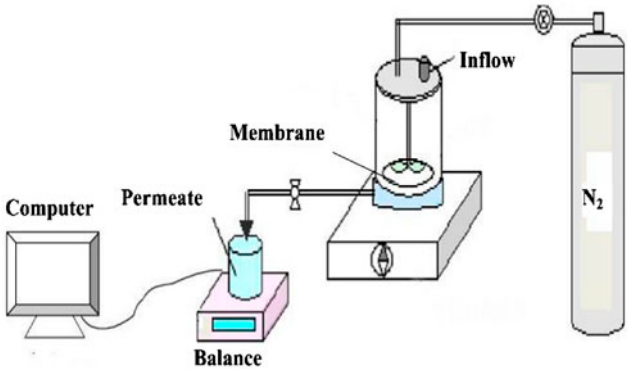

Fig. 1. Schematic of membrane filtration set-up.

2.4. Analytical technology

The DOC was used to reflect the concentration of dissolved organic matter in different wastewater samples and was determined using a total organic carbon (TOC) analyser (TOC-L, CPN, Shimadzu Japan). A Hitachi high-performance liquid chromatograph (LC-2000, Japan) equipped with a gel column (Waters Ultrahydrogel 250) was used to analyse the molecular weight distribution of each sample using ultraviolet light as detector. Poly(styrenesulfonate) samples with molecular weights of 77, 17 and 4.3 kDa, and acetone dissolved in Milli-Q water were used as standards for calibration. The mobile phase was 0.05 mol/L sodium acetate solution. The flow rate was 0.6 ml/L and a sample injection volume of 25 μL was used. The surface morphology of clean and fouled membranes was analysed using a Multimode 8.0 AFM (Bruker, Germany) with NanoScope V controller (Bruker) and manufacturer-supplied software. All measurements were performed under contact mode in air. A silicon nitride SNL-10 (Bruker) probe with a spring constant of 0.24 N/m was used in this study. The scan area was 5×5 μm.

3. Results and discussion

3.1. Changes in membrane morphology

Fig. 2 shows AFM images of clean and fouled membranes. The clean membrane displayed a homogeneous porous surface structure. For each fouled membrane, a cake layer was formed on the membrane surface. However, the surface morphologies of BSA-, SA-, HA- and EfOM-fouled membranes differed. Compared with other fouled membranes, the gel layer on the HA membrane surface appeared to be looser and more porous. For the SA-fouled membrane, the membrane surface was relatively less porous, but seemed to be slightly looser. The EfOM-fouled-membrane surface had not been completely

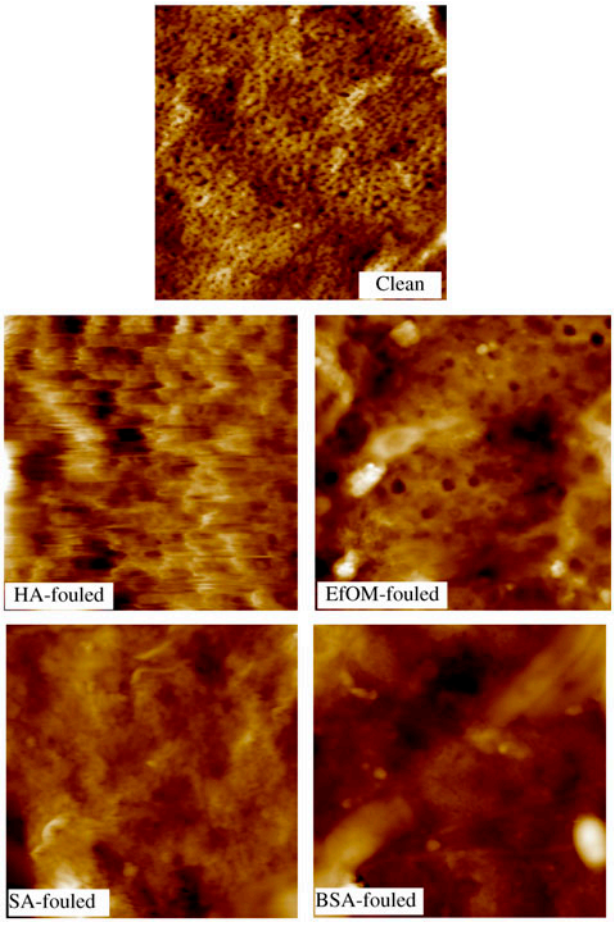

Fig. 2. AFM images of clean and fouled membrane. The scan area = 5 × 5 μm. Fouling filtration time = 2 h.

covered by foulants and although there were obvious pores on the membrane surface, its gel layer looked more compact than those for HA- and SA-fouled membranes. For the BSA-fouled membrane, most of the surface pores were covered by foulants and its gel layer seemed to be more compact. The above conclusions could be further confirmed by the surface roughness of the fouled membranes.

The average roughness of membranes fouled by BSA, HA, SA and EfOM was 45.5, 70.1, 65.3 and 61.7 nm, respectively. It is clear that there was a close relationship between surface roughness and the structure of the gel layer—the more compact the gel layer, the lower its surface roughness. However, it should be noted that the surface roughness of a clean membrane was merely 15.3 nm, which is far smaller than that of all fouled membranes. The increase in surface roughness of fouled membranes may be attributed to the accumulation of large macromolecular foulants on their surface [26].

3.2. Molecular weight distribution of feed solution and permeate analysis

The molecular weight distributions of the feed solutions and permeates of SA, HA and EfOM are shown in Fig. 3. The chromatogram of BSA samples is not included because of its fixed molecular weight (M_w = 67 kDa). It can be seen from Fig. 3 that most M_w of samples are lower than 10 kDa and the M_w distribution of HA, SA and EfOM is very similar. There is an evident decline in peak intensity of 0.5–4.0 kDa in the EfOM permeate. Compared with the feed solutions of SA and HA, the intensity of the peak of 4.1–4.2 kDa declined significantly in the respective permeates. On the whole, the filtration experiments did not cause significant changes in the M_w distribution of EfOM, SA and HA, and excluding a few macromolecular foulants, removal of small molecular substances in wastewater by UF membranes is difficult. This is well explained by the studies of Wang et al. who found that substances in the large M_w range could be rejected in significant amounts by membranes and accumulate on membrane surfaces, which in turn cause membrane fouling [27].

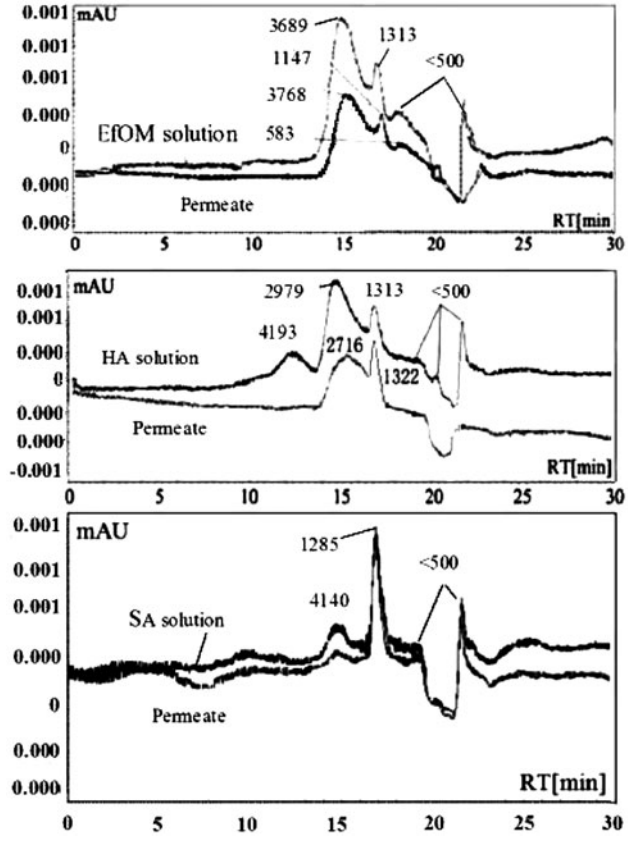

Fig. 3. Molecular weight distribution of feed solution and permeate for SA, HA and EfOM foulants.

In contrast, the substances in the relatively smaller M_w range could penetrate through pores and the gel layer [28]. However, we could observe that most of the organic materials in the secondary wastewater effluent were small molecular substances.

3.3. Membrane fouling experiments

Fig. 4 presents the variation in the flux during the fouling period. To avoid the concentration effect, each kind of feed solution was diluted to the same DOC level of 6.4 mg/L. The results clearly show that the flux decline rate and extent of HA-fouled membrane were at a minimum over the whole fouling period compared with other fouled membranes. For SA-, BSA- and EfOM-fouled membranes, there is a significant flux decline rate and extent in the initial filtration stage, while the flux decline rate and extent of SA-, BSA- and EfOM-fouled membranes in the later filtration stage are very gradual. Further, in the initial filtration stage, the flux decline rate and extent of the three kinds of fouled membranes follow the order EfOM < SA < BSA. These discrepancies may be attributed to the difference between membrane–foulant interactions, which was considered as the major factor to control membrane fouling [29]. However, in the later filtration stage, the flux decline rate and the extent of the SA-fouled membrane were more severe than those of BSA-fouled membranes. The flux profiles of BSA- and EfOM-fouled membranes were equivalent. These changes could be attributed to the variation in the leading position of membrane–foulant and foulant–foulant interactions at different filtration stages. That is, in the initial filtration stage, the deposition of foulants on the membrane surface was controlled by the interaction between the bulk foulants and the membrane surface. With the accumulation of foulants on the membrane surface, the fouling behaviour is controlled by the interactions between bulk foulants and the foulants deposited on the membrane surface [30]. Thus, for EfOM-, SA- and BSA-fouled membranes, there were significant differences between their flux decline order in the initial and later filtration stages. On the other hand, it is worth noting that the flux of the BSA-fouled membrane declined by almost 70% in less than 10 min of filtration, which is much higher than the flux decline extent of HA-, SA- and EfOM-fouled membranes at the same filtration stage. This phenomenon could be explained by the differences in molecular weight distribution of BSA, SA, HA and EfOM (Fig. 3). Most molecular weights of SA, HA and EfOM were lower than 10 kDa, whereas that of BSA was 67 kDa. Macromolecular BSA resulted in the fast blocking of membrane pores and even in higher flux decline rate and extent.

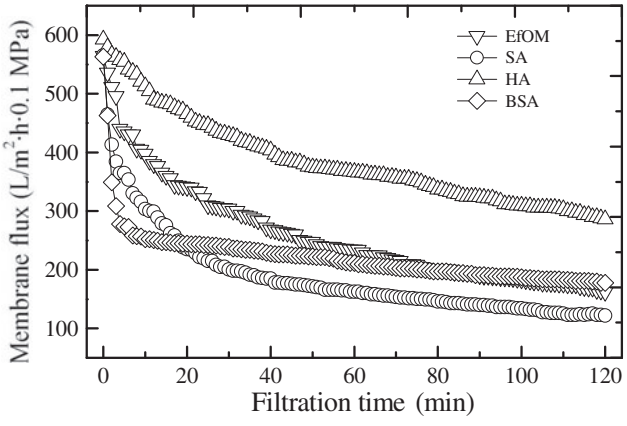

Fig. 4. Variation of the flux during the fouling period. Other experiments conditions: DOC of BSA, SA, HA and EfOM = 6.4 mg/L, and applied pressure = 0.1 MPa.

Combined with the analysis of AFM images in section 3.1, it appears that the membrane fouling behaviour was closely associated with the structure of the gel layer on the fouled-membrane surface. The gel layer on the HA-fouled membrane was seen to be looser and more porous, and the flux decline rate and extent of HA-fouled membrane were not significant; on the other hand, for the BSA- and SA-fouled membranes, these properties were almost the opposite.

Comparing the flux decline profiles of BSA-, SA-, HA- and EfOM-fouled membranes, it is easy to see that the flux decline profile of the EfOM-fouled membrane was not completely identical with that of any of the BSA-, SA- or HA-fouled membranes, indicating that it is difficult to simulate the fouling behaviour of complex actual wastewater by a single model foulant.

Furthermore, the extent of flux decline of the BSA-, SA-, HA- and EfOM-fouled membranes was more than 50% during the 0–40 min filtration period, and the flux decline rate became very gradual in the later filtration stage (less than 10%). It was clearly shown that membrane fouling was more likely to occur in the initial rather than in the later filtration stage. This phenomenon is consistent with the previous observation that the membrane flux decline rate and extent are dominantly governed by the interaction between membrane and foulants in the initial membrane filtration stage [29].

3.4. DOC removal rate analysis

The DOC values of the feed solution and permeate were collected at different filtration times and are depicted in Fig. 5. It was surprising to find that the DOC removal rate of the HA-fouled membrane

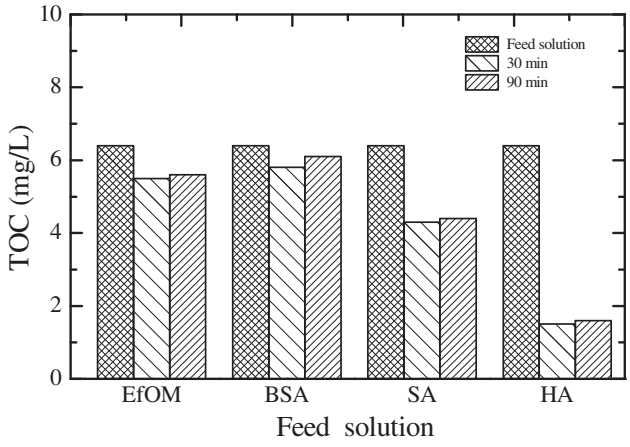

Fig. 5. The DOC of feed solution and permeate in different stages of fouling filtration.

reached 80%, whereas that for the BSA-fouled membrane was less than 10%. This phenomenon did not correspond well to the flux decline profiles of HA- and BSA-fouled membranes. A possible explanation would be the large differences between the molecular structures of BSA and HA. The HA molecules could cross-link with each other to form a porous and mesh gel layer. The cross-linked molecular structure would be well rejected by the membrane, and the porous and mesh gel layer would result in a gentle flux decline rate. In contrast, the ellipsoidal-shaped BSA [31] could not cross-link and would pass more easily through the membrane surface, resulting in a low DOC removal rate. However, the molecular weight of BSA is 67 kDa, which could cause severe pore plugging in the initial stage of fouling and a sharp flux decline. Further research needs to confirm this conclusion. It is worth noting that the DOC of the permeate increased slightly with filtration time. The increases in DOC of all permeate samples might be mainly caused by concentration polarization in the membrane surface. Moreover, the DOC removal rate of secondary wastewater effluent by the UF membrane was less than 10%. This phenomenon was readily reflected in the changes in the molecular weight distribution of the feed solution and permeate of EfOM.

4. Conclusions

To reveal the fouling behaviour of PVDF UF membranes by SA, HA, BSA and EfOM, a series of laboratory-scale fouling experiments were conducted and the performance of feed solution, permeate, clean and fouled membranes was investigated. Based on this study, the following conclusions can be drawn.

(1) AFM images indicated a significant effect of the foulant type on the surface morphology of the gel layer. In addition, the fouled-membrane surface roughness was closely related to the structure of the gel layer. This phenomenon was more obvious in BSA- and HA-fouled membranes. For the HA-fouled membrane, a porous and loose gel layer formed on the surface, which resulted in higher surface roughness. For the BSA-fouled membrane, the gel layer on the membrane surface was more compact and the surface roughness was lower.
(2) In molecular weight distribution analyses, it was found that the largest proportion in the SA, HA and EfOM feed solution was taken by molecular weights below 10 kDa, which was far below the molecular weight of BSA ($M_w = 67$ kDa). Filtration experiments did not cause significant changes in the molecular weight distribution of these solutions. It was also found that the UF membranes used in this study have barely any removal efficiency for small molecular substances.
(3) The results of fouling experiments showed that the fouling behaviours of BSA-, SA-, HA- and EfOM-fouled membranes were different. None of the single foulants (BSA, SA and HA) could completely simulate the fouling behaviour of complex actual wastewater (EfOM). Furthermore, membrane fouling mainly occurred in the initial filtration stage, that is, membrane flux decline rate and extent were dominantly governed by the interactions between membrane and foulants. Combined with the AFM images, it was clear that there was a strong correlation between flux decline rate and the structure of the gel layer on fouled membranes. In addition, membrane fouling was mainly caused by macromolecular foulants, which was well reflected by the molecular weight differences of the feed solution and permeate.
(4) The DOC removal rate showed that small molecule foulants in wastewater are difficult to remove by the UF membrane. However, further research is needed to confirm the phenomenon that the DOC removal rate of HA is the highest and the flux decline rate of the HA-fouled membrane is the lowest.

Conflict of interest statement

The authors declare no competing financial interest.

Acknowledgments

Financial support for this study was provided by the National Natural Science Foundation of China (Grant Nos. 51178378, 51278408 and 51008243), the Shanxi Province Science and Technology Innovation Projects (Grant No. 2012KTCL03-06) and the Foundation of Shanxi Educational Committee (Grant No. 2013JK0884).

References

[1] G.K. Pearce, Fouling behaviour for different module formats in membrane filtration applications for surface water treatment, Desalin. Water Treat. 8 (2009) 48–53.
[2] S. Pourjafar, A. Rahimpour, M. Jahanshahi, Synthesis and characterization of PVA/PES thin film composite nanofiltration membrane modified with TiO_2 nanoparticles for better performance and surface properties, J. Ind. Eng. Chem. 18 (2012) 1398–1405.
[3] N. Lee, G. Amy, J.P. Croué, H. Buisson, Identification and understanding of fouling in low-pressure membrane (MF/UF) filtration by natural organic matter (NOM), Water Res. 38 (2004) 4511–4523.
[4] C.W. Jung, H.J. Son, Evaluation of membrane fouling mechanism in various membrane pretreatment processes, Desalin. Water Treat. 2 (2009) 199–208.
[5] H.K. Shon, S. Vigneswaran, S. Kim, J. Cho, H.H. Ngo, Fouling of ultrafiltration membrane by effluent organic matter: A detailed characterization using different organic fractions in wastewater, J. Membr. Sci. 278 (2006) 232–238.
[6] X. Bernat, G. Prats, B. Lefèvre, O. Gibert, J. Tobell, Membrane fouling characterization and cleaning adaptation in wastewater reclamation plants: From plant to lab, Desalin. Water Treat. 34 (2011) 361–366.
[7] M. Hashino, K. Hirami, T. Katagiri, N. Kubota, Y. Ohmukai, T. Ishigami, T. Maruyama, H. Matsuyama, Effects of three natural organic matter types on cellulose acetate butyrate microfiltration membrane fouling, J. Membr. Sci. 379 (2011) 233–238.
[8] K.S. Katsoufidou, D.C. Sioutopoulos, S.G. Yiantsios, A.J. Karabelas, UF membrane fouling by mixtures of humic acids and sodium alginate: Fouling mechanisms and reversibility, Desalination 264 (2010) 220–227.
[9] H.-C. Kim, B.A. Dempsey, Effects of wastewater effluent organic materials on fouling in ultrafiltration, Water Res. 42 (2008) 3379–3384.
[10] M. Rebhun, J. Manka, Classification of organics in secondary effluents, Environ. Sci. Technol. 5 (1971) 606–609.
[11] T. Tran, B. Bolto, S. Gray, M. Hoang, E. Ostarcevic, An autopsy study of a fouled reverse osmosis membrane element used in a brackish water treatment plant, Water Res. 41 (2007) 3915–3923.
[12] N. Her, G. Amy, A. Plottu-Pecheux, Y. Yoon, Identificati of nanofiltration membrane foulants, Water Res. 41 (2007) 3936–3947.
[13] Y.J. Chang, M.M. Benjamin, Modeling formation of natural organic matter fouling layers on ultrafiltration membranes, J. Environ. Eng. 129 (2003) 25–32.
[14] S. Lee, W.S. Ang, M. Elimelech, Fouling of reverse osmosis membranes by hydrophilic organic matter: Implications for water reuse, Desalination 187 (2006) 313–321.
[15] K. Kimura, Y. Hane, Y. Watanabe, G. Amy, N. Ohkuma, Irreversible membrane fouling during ultrafiltration of surface water, Water Res. 38 (2004) 3431–3441.
[16] K. Kimura, H. Yamamura, Y. Watanabe, Irreversible fouling in MF /UF membranes caused by natural organic matters (NOMs) isolated from different origins, Sep. Sci. Technol. 41 (2006) 1331–1344.
[17] S. Liang, C. Liu, L.F. Song, Soluble microbial products in membrane bioreactor operation: Behaviors, characteristics, and fouling potential, Water Res. 41 (2007) 95–101.
[18] S. Arabi, G. Nakhla, Impact of protein/carbohydrate ratio in the feed wastewater on the membrane fouling in membrane bioreactors, J. Membr. Sci. 324 (2008) 142–150.
[19] K. Katsoufidou, S.G. Yiantsios, A.J. Karabelas, A study of ultrafiltration membrane fouling by humic acids and flux recovery by backwashing: Experiments and modeling, J. Membr. Sci. 266 (2005) 40–50.
[20] G. Amy, Fundamental understanding of organic matter fouling of membranes, Desalination 231 (2008) 44–51.
[21] H. Susanto, H. Arafat, E.M.L. Janssen, M. Ulbricht, Ultrafiltration of polysaccharide-protein mixtures: Elucidation of fouling mechanisms and fouling control by membrane surface modification, Sep. Sci. Technol. 63 (2008) 558–565.
[22] D.-J. Lin, H.-H. Chang, T.-C. Chen, Y.-C. Lee, L.-P. Cheng, Formation of porous poly(vinylidene fluoride) membranes with symmetric or asymmetric morphology by immersion precipitation in the water/TEP/PVDF system, Eur. Polym. J. 42 (2006) 1581–1594.
[23] X.R. Meng, L. Zhao, L. Wang, X.D. Wang, D.X. Huang, R. Miao, Study of antifouling modified ultrafiltration membrane based on the secondary treated water of urban sewage, Water Sci. Technol. 66 (2012) 2074–2082.
[24] X.D. Wang, L. Wang, Y. Liu, W.S. Duan, Ozonation pretreatment for ultrafiltration of the secondary effluent, J. Membr. Sci. 287 (2007) 187–191.
[25] C.C. Ho, A.L. Zydney, A combined pore blockage and cake filtration model for protein fouling during micro filtration, J. Colloid Interface Sci. 232 (2000) 389–399.
[26] Y. Shen, W. Zhao, K. Xiao, X. Huang, A systematic insight into fouling propensity of soluble microbial products in membrane bioreactors based on hydrophobic interaction and size exclusion, J. Membr. Sci. 346 (2010) 187–193.
[27] P. Wang, Z.W. Wang, Z.C. Wu, S.H. Mai, Fouling behaviours of two membranes in a submerged membrane bioreactor for municipal wastewater treatment, J. Membr. Sci. 382 (2011) 60–69.
[28] Z.W. Wang, Z.C. Wu, X. Yin, L.M. Lu, Membrane fouling in a submerged membrane bioreactor (MBR) under sub-critical flux peration: Membrane foulant and gel layer characterization, J. Membr. Sci. 325 (2008) 238–244.
[29] M. Hashino, K. Hirami, T. Ishigami, Y. Ohmukai, T. Maruyama, N. Kubota, H. Matsuyama, Effect of kinds of membrane materials on membrane fouling with BSA, J. Membr. Sci. 384 (2011) 157–165.
[30] S.Y. Lee, M. Elimelech, Relating organic fouling of RO membranes to intermolecular adhesion forces, Environ. Sci. Technol. 40 (2006) 980–987.
[31] Q. She, C. Tang, Y.N. Wang, Z. Zhang, The role of hydrodynamic conditions and solution chemistry on protein fouling during ultrafiltration, Desalination 249 (2009) 1079–1087.